Electronic supplementary information (ESI) for

Nanodiamond: a critical component in anode for high performance lithium-ion battery

Yanpeng Song,[a] Hongdong Li,*[a] Liying Wang,[a] Dongchao Qiu,[a,c] Yibo Ma,[a] Kai Pei,[a] Guangtian Zou,[a] and Kaifeng Yu*[b]

[a]State Key Laboratory of Superhard Materials, Jilin University, Changchun 130012, PR China

E-mail: hdli@jlu.edu.cn

[b]College of Materials Science and Engineering, Jilin University, Changchun 130025, PR China

E-mail: yukf@jlu.edu.cn

[c]School of Science, Liaoning University of Science and Technology, Anshan 114051, PR China

Synthesis of GNSs and DND/GNSs powders: The precusors of citric acid (2 g), urea (6 g) and DNDs (0~160mg) were dispersed in deionized water (30 mL). After treated by a ultrasonic processing, the suspension was heated in a domestic 850 W microwave oven at 2.45 GHz for 10~15 mins in atmosphere ambient. The porous solid powers were transferred to a vacuum oven and heated at 60 °C for 1 h to remove the residual small molecules. The products were then put into a tube furnace calcinating at 900 °C in an argon atmosphere for 2 h. Finally, the GNS and DND/GNS powders were obtained by grinding.

Characterizations: The morphology and structure of the samples were characterized by means of a scanning electron microscope (SEM, JEM-6700F, JEOL), a field-emission transmission electron microscope (TEM, JEM-2200FS, JEOL), X-ray diffraction (XRD, XRD-6000, Shimadzu) with Cu Kα radiation, Raman spectroscopy (Renishaw in Via) with argon-ion excitation laser at 514.5 nm. The specific surface area of the CNS and DND/CNS powders were measured using nitrogen adsorption-desorption measurements (Micromeritics, ASAP 2420). Fourier transform infrared spectroscopy (FTIR) was performed using a Bruker Optics - IFS 66v/S Vacuum FT-IR spectrometer.

Preparation and electrochemical characterizations of electrodes and Li-ion batteries: The working electrodes consisted of active material (GNSs, DND/GNSs), carbon black and polymer binder (polyvinylidene fluodide, PVDF) in a weight ratio of 80: 10: 10. The powders were further mixed in N-methyl-2-pyrrolidone (NMP) and stirred for at least 10 h until the paste reached a smooth syrupy viscosity. The mixed slurry was coated on a copper foil. After drying at 120 °C in a vacuum oven for 12 h, the circular discs were punched out with 10 mm in diameter. The average mass of active materials in the circular disc is about 0.8 mg, and the area mass density of active materials in electrode is about 1 mg cm^{-2}. The fabricated carbon electrodes were coupled with a lithium foil (as the counter and reference electrodes) in a coin cell, with a 1 mol L^{-1} solution of $LiPF_6$ in a 1:1 (v/v) mixture of ethylene carbonate and diethyl carbonate (EC–DEC). The electrochemical characterization was carried out using 2025 type coin cells. The cell assembly was performed in an Ar-filled glove box with moisture and oxygen concentrations below 1.0 ppm. The charge and discharge performance of the half-cells was tested with a LAND cycler (Wuhan, China) at room temperature. The half-cells were cycled at 0.2 C in the voltages range between 0.02 V and 3 V. Galvanostatic charge–discharge profiles were recorded between 0.02 V and 3.0 V at a 0.2 C (1 C = 372 mA hg^{-1}) rate on the LAND multi-channel battery tester. Cyclic voltammetry (CV) and Electrochemical impedance spectroscopy (EIS) measurements were implemented on a electrochemical workstation (CHI-614D, CHI Shanghai).

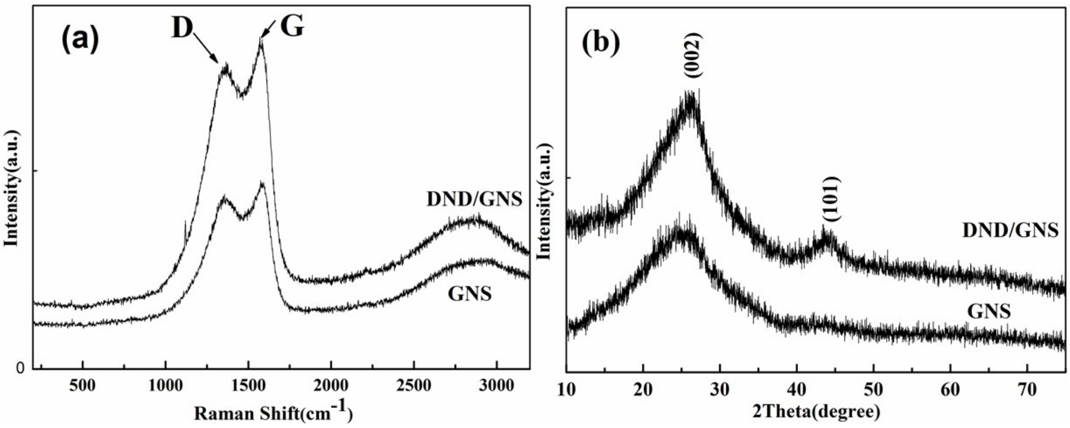

Fig. S1 – (a) Raman spectroscopy and (b) XRD pattern of DND/GNS and GNS powders.

In the Raman spectra of the GNSs and DND/GNSs, the Raman peaks centered at 1350 cm^{-1} and 1580 cm^{-1} can be attributed to the D and G bands of graphitic structure, respectively. The broad peak at 2800 cm^{-1} is an overtone of D band. In Raman spectra, the diamond peak at ~1332 cm^{-1} is not obvious, because the amount of DNDs in the samples is small. The XRD results show the similar pattern of GNS and DND/GNS samples. The broad peaks centered at 26° and 43° are assigned to the (002) and (101) diffraction peaks of hexagonal graphite.

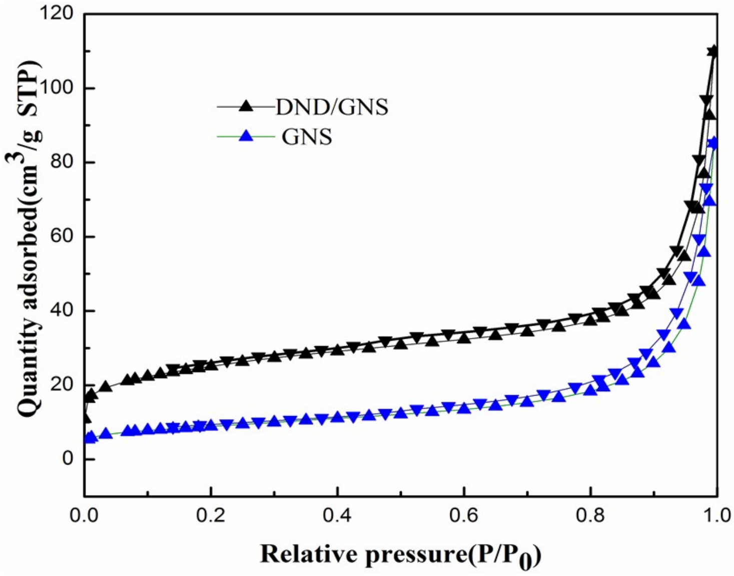

Fig. S2 –N_2 adsorption-desorption isotherms of DND/GNS and GNS powders.

The nitrogen adsorption-desorption isotherm curves represent a typical type-IV isotherm with an associated H4-type hysteresis loop. The calculated specific surface area of the DND/GNS (with 1.25 wt% DNDs) powder is about 87.2 m^2g^{-1}, which is higher than that of the GNS powder (31.4 m^2g^{-1}).

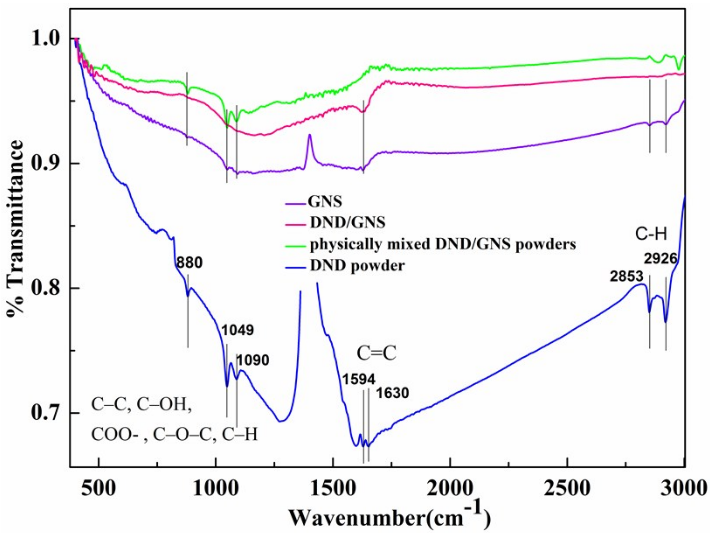

Fig. S3 –FTIR spectra of DND powder, fabricated GNS, active anode of DND/GNS, and physically mixed GNS and DND powders.

Fourier transform infrared spectroscopy (FTIR) spectra were proposed to study the surface features of the related materials (pressed into plates mixed with KBr powder), including the DND powder, fabricated GNS, active anode material of DND/GNS, and the mechanically (physically) mixed raw DND and the fabricated GNS powders. It is found that except the case of the active GNS/DND, the absorption bands obtained from the other three samples are similar appearing in the wavenumber region of 700–3000 cm^{-1}, originating from surface radicals, such as C–C, C=C, C–OH, COO−, C–O–C, and/or C–H on the isolated DND (GNS), and physically mixed DND/GNS. Importantly, for the fabricated hybrid DND/GNS as anode material, those absorption peaks related surface radicals nearly disappear, and the band centered at 1600 cm^{-1} to the C=C bonding become strong, implying that the bonding between DND and GNS would be significantly different to the above physically mixed DND/GNS. In fact, taking into account the fabrication process of hybrid DND/GNS, i.e., thermally heated by microwave oven, vacuum drying, annealing at 900 ^{o}C in Ar ambient, and then make full grinding, the formation of chemical bonding between DND and GNS is thus reasonable.

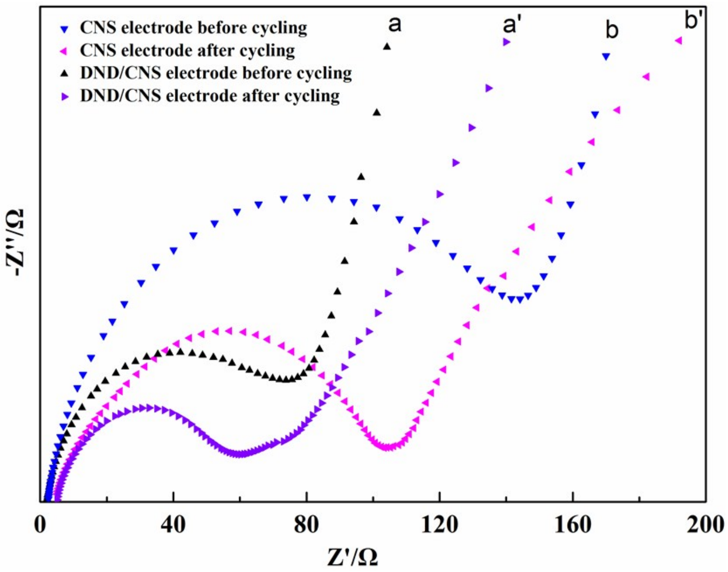

Fig. S4 –Impedance plots of the as-synthesized (a and b) and after 5 circles (a'and b') for the electrodes made from DND/GNS and GNS.

The typical Nyquist plots of electrochemical impedance spectroscopy (EIS) show the impedance profiles of the DND/GNS and GNS electrodes before and after circling (5th circle). The diameters of the semicircles for DND/GNS electrode before and after circling are smaller than that for the GNS electrode, meaning that the charge transfer resistances of the DND/GNS are lower than that of the GNS electrode. The improvement in the electrochemical performance of the hybrid DND/GNS structure can be attributed to good electrical contact between the matrix and active material, and the formation of stable solid electrolyte interface (SEI) which can prevent the electrolyte decomposition on the active electrode. In addition, the high density DNDs provide more storage positions and decrease the path length for Li ions transportation. The hybrid DND/GNS anode thus enhance the performance of lithium ion battery, as discussed in the text.

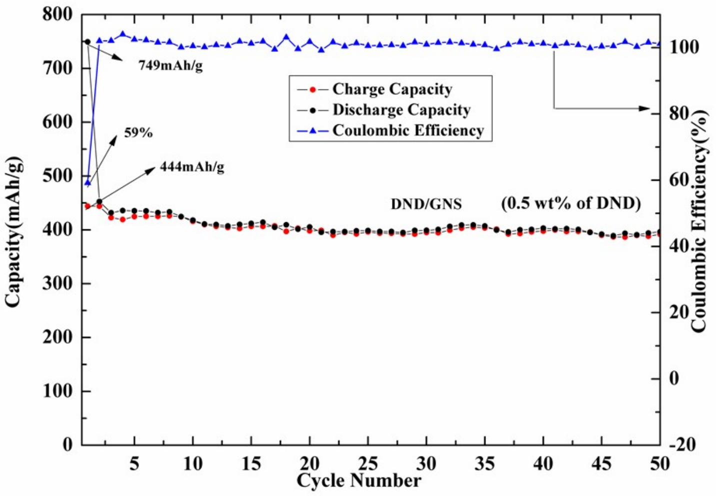

Fig. S5 –Cycling performance profiles at a rate of 0.2 C of DND/GNS electrode with 0.5 wt % of DND

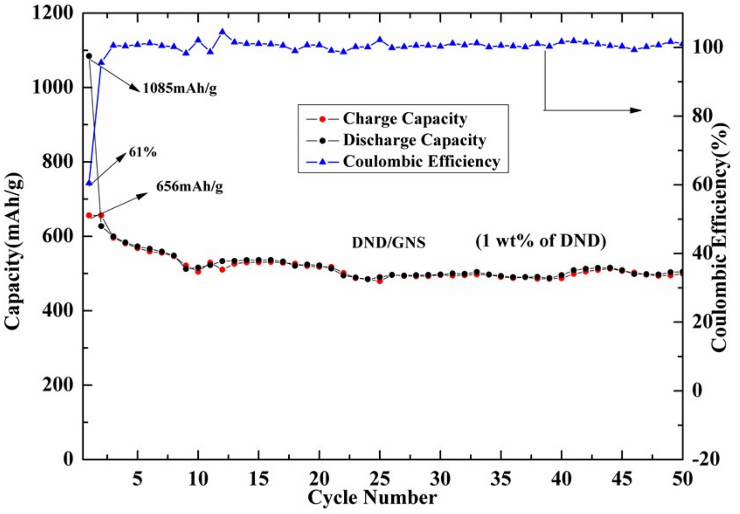

Fig. S6 –Cycling performance profiles at a rate of 0.2 C of DND/GNS electrode with 1 wt % of DND

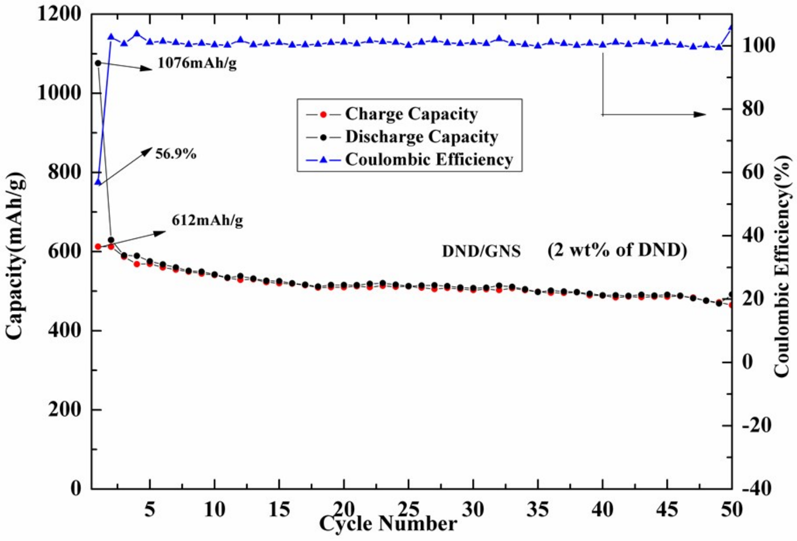

Fig. S7 –Cycling performance profiles at a rate of 0.2 C of DND/GNS electrode with 2 wt % of DND